ISSN 1392-1207. MECHANIKA. Vol. 29, No. 4, 2023: 317–323

An Energy-Based Anti-Fatigue Optimization Design Method of Welded Rear Axle Housing in a Mining Dump Truck

Chengji MI*, Yongqiang LI, Chen ZHANG***, Dong ZHANG****, Xianghuan LIU*****, Xiaolan HU******, Dejun ZHANG*******

**Department of Mechanical Engineering, Hunan University of Technology, Zhuzhou, 412007, China, E-mail: michengji_86@126.com*
***Department of Mechanical Engineering, Hunan University of Technology, Zhuzhou, 412007, China, E-mail: happy2021hut@126.com*
****Department of Mechanical Engineering, Hunan University of Technology, Zhuzhou, 412007, China, E-mail: zhangchen@126.com*
*****Department of Mechanical Engineering, Hunan University of Technology, Zhuzhou, 412007, China, E-mail: zhangdong@126.com*
******Zhuzhou Gear Co. Ltd, Zhuzhou, 412007, China, E-mail: liuxianghuan@126.com*
*******Zhuzhou Gear Co. Ltd, Zhuzhou, 412007, China, E-mail: huxiaolan@126.com*
********Zhuzhou Gear Co. Ltd, Zhuzhou, 412007, China, E-mail: zhangdejun@126.com*

https://doi.org/10.5755/j02.mech.32371

1. Introduction

Considered as the bearing part in the mining dump truck, the rear axle housing often suffers from local fatigue cracking due to cyclic loading [1, 2]. The rear axle housing is mostly welded by high-strength steel plate. The traditional empirical design will result in problems such as stress concentration and fatigue life shortage, which will lead to the cracking at the welding toe [3]. Due to the complex geometry, random load and complex damage mechanism of the rear axle housing, it is difficult to exactly calculate the fatigue life through the traditional fatigue model.

Usually, the crack starts from the weld toe because of the stress concentration, so that the nominal stress is mostly considered as the damage parameter to evaluate the fatigue life of welded structure [4, 5]. However, the stress calculation of welded structure under complex loads focuses on the elastic stage, which ignores the fatigue damage caused by plastic deformation. Based on the local stress-strain method, the finite element analysis is used to determine the parameters in the fatigue expectancy prediction models [6]. The above-mentioned method is constructed on the continuum damage mechanics theory, but sometimes there are micro-cracks or defects in the welded part. The fracture mechanics method can estimate the lifetime of the welded structure with pre-cracks, but it is hard to solve the plastic constraint and crack closure effect on the surface of welded structure [7, 8]. The both stress and strain damage parameters are vector, and it often takes a lot of time to make sure the direction [9, 10]. Therefore, the energy-based fatigue life prediction method is presented in this paper.

Some researchers tried to estimate the fatigue life of axle housing by use of the test and simulation. The overall fatigue life distribution of the axle housing was obtained from the simulated results under compression-tension loading or random loading, and compared with the data from the bench fatigue tests [11-13]. According to the dynamic stress test of real vehicle, the local stress concentration had a great influence on fatigue life of weak region [14-15]. However, how to effectively and accurately improve the lifetime of axle housing is still a challenging work.

In this paper, an energy-based fatigue life estimation method of rear axle housing was presented. Then, the stress and strain of rear axle housing under cyclic loadings was obtained through finite element analysis. After the minimum lifetime of welded rear axle housing was evaluated to be insufficient, the anti-fatigue optimization based on the multi-island genetic algorithm was conducted.

2. Strain energy density method

The strain energy density includes two parts, and the elastic strain energy density ΔW_{e+} and plastic strain energy density ΔW_P are generated during cyclic loading of welded joints. ΔW_P is obtained by calculating the area of the hysteresis loop, while ΔW_P is mainly determined by the maximum equivalent stress [3], as shown in Fig. 1.

The tensile positive elastic strain energy density is calculated as [3]:

$$\Delta W_{e+} = \frac{\sigma_{max}^2}{2E}, \tag{1}$$

where: σ_{max} is the maximum tensile stress; E is the elastic modulus.

The plastic strain density could be expressed as [3]:

$$\Delta W_P = \int_{\varepsilon_P^{min}}^{\varepsilon_P^{max}} \sigma d\varepsilon_P, \tag{2}$$

where: σ is stress; ε_P is plastic strain; ε_P^{max} and ε_P^{min} are the maximum and minimum plastic strain, respectively.

The total strain energy density is sum of the plastic strain energy and the tensile positive elastic strain energy density, and its relationship with fatigue life can be

shown as follows [3]:

$$\Delta W^t = \Delta W^{e+} + \Delta W^P = A\left(2N_f\right)^B, \quad (3)$$

where: N_f is the fatigue life; A is the strain energy density coefficient; B is the strain energy density index.

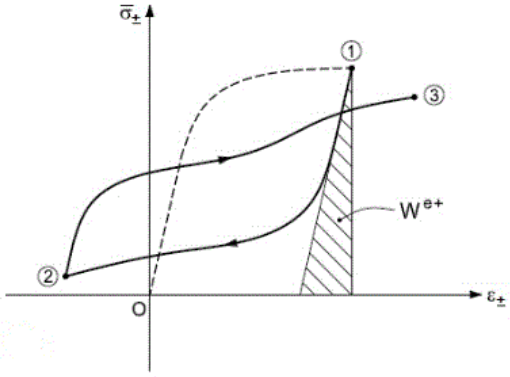

a

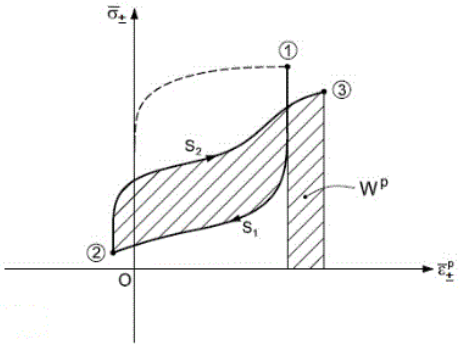

b

Fig. 1 Calculation of strain energy density under cyclic loading: a) elastic part; b) plastic part

3. Fatigue life prediction of welded rear axle housing

3.1. Finite element model

The rear axle housing is connected by different thickness high strength steel plates through arc welding. In order to improve the computational efficiency, some process features were simplified and some small holes were removed. The geometric model of rear axle housing was re-established, as shown in Fig. 2.

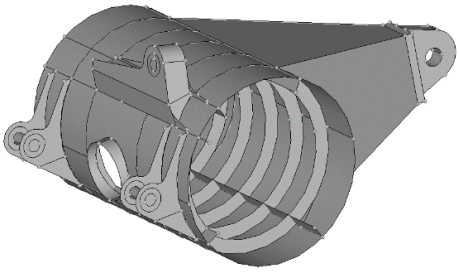

Fig. 2 Geometric model of rear axle housing

Software Hypermesh was utilized to build the finite element model of rear axle housing, and it had 28836 elements, consisting of a mixture of triangular and quadrilateral elements, as well as 27436 nodes. The complete grid model was shown in Fig. 3. The yellow and red elements in Fig. 3 were considered as the welded seam.

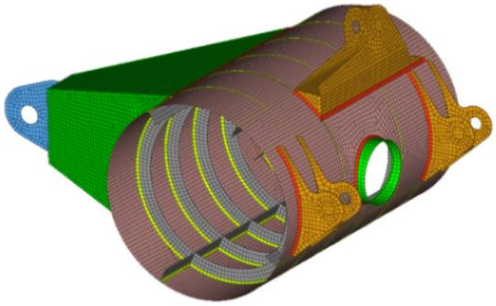

Fig. 3 Finite element model of rear axle housing

The rear axle housing was welded by different thickness plates, and the parental material was high strength steel HQ60. Its elastic modulus is 210 GPa, the Poisson's ratio is 0.28, the density is 7.85×10^3 kg/m^3, the yield limit is 500 MPa, and the strength limit is 600 MPa. The mechanical parameters of the welded joints were close to the parental material [3].

In order to ensure the accuracy and effectiveness of the finite element model, the simulated stress under full load at the speed of 25 km/h was compared with the tested data on the mine road surface, as shown in Fig. 4. The tested points were shown in Fig. 5, and one pasted strain gauge was displayed in Fig. 6.

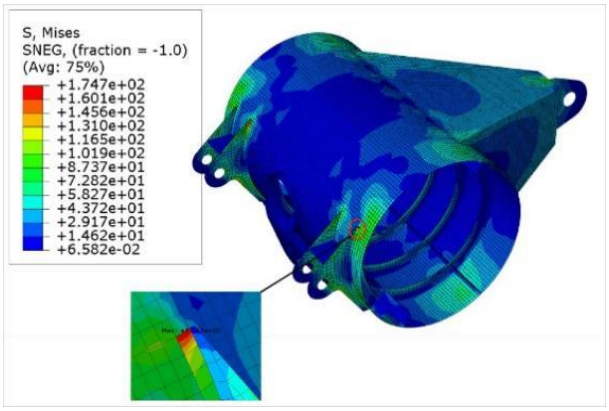

Fig. 4 Stress contour under full load

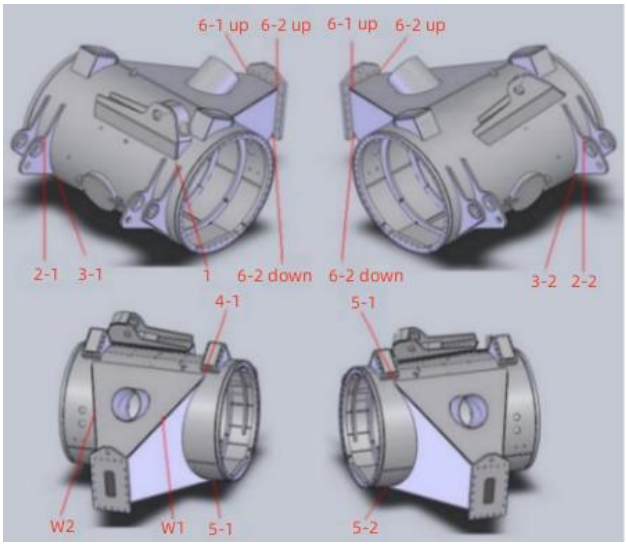

Fig. 5 Layout diagram of tested points

Fig. 6 Installation diagram of strain gauge

Once the strain history along three directions was recorded, respectively, the principal stress could be calculated from the following equation [3]:

$$\sigma_i = \frac{E}{2(1-\mu)}(\varepsilon_a + \varepsilon_c) \pm \\ \pm \frac{E}{\sqrt{2}(1+\mu)}\sqrt{(\varepsilon_a - \varepsilon_b)^2 + (\varepsilon_b - \varepsilon_c)^2} \quad , \qquad (4)$$
$$\tau_{max} = \frac{\sqrt{2}E}{2(1+\mu)}\sqrt{(\varepsilon_a - \varepsilon_b)^2 + (\varepsilon_b - \varepsilon_c)^2}$$

where: E is the elastic modulus; μ is Poisson's ratio; ε_a, ε_b, ε_c is the strain history in the three directions, respectively. σ_i is the principal stress, and τ_{max} is the maximum shear stress.

The tested results and simulated ones were shown in Table 1. The maximum stress was located at point 3-2, which was at the root of the left ear plate in right rear suspension support system. All the error of tested points was within 10%, except the point 1. This may be caused by the omitting the lateral force at the rear stabilizer bar in the simulation. However, the accuracy of finite element model was acceptable.

Table 1

Comparison of stress at tested points

Type	1	2-1	2-2	3-1	3-2	4-1	4-2	5-1	5-2	6-1 up	6-2 up	6-1 down	6-2 down	W1	W2
Tested data, MPa	24.3	55.2	39.3	64.8	64.9	45.3	39.5	58.0	57.7	22.7	20.1	27.9	28.2	34.1	35.0
Simulated results, MPa	19.5	51.9	41.1	61.8	60.3	42.5	37.3	55.8	52.9	20.2	18.6	26.2	26.5	33.2	37.2
Error, %	19.7	5.9	-4.5	4.7	7.2	6.2	5.7	3.9	8.3	1.1	7.5	6.1	6.0	2.5	-6.3

3.2. Multi-load step finite element analysis

In order to estimate the fatigue life of welded rear axle housing, the stress and strain under cyclic loadings had to be firstly determined. The finite element analysis was conducted on the welded rear axle housing, and the load history was obtained from the multi-body dynamic analysis under full load at the speed of 25 km/h on the surface of potholed pavement [17]. However, the load history had to be simplified into three loading steps, namely loading-unloading-reloading [3]. The equivalent load in the vertical direction at left rear suspension was shown in Fig. 7. The other loads also coped with like this. The side edge of welded rear axle housing was fixed, and the connection parts between rear axle housing and frame and at the rear suspension support were applied cyclic loadings. Then, the stress and strain under full load at the speed of 25 km/h on the surface of potholed pavement and 17% slope turning pavement was shown in Figs. 8 and 9 respectively.

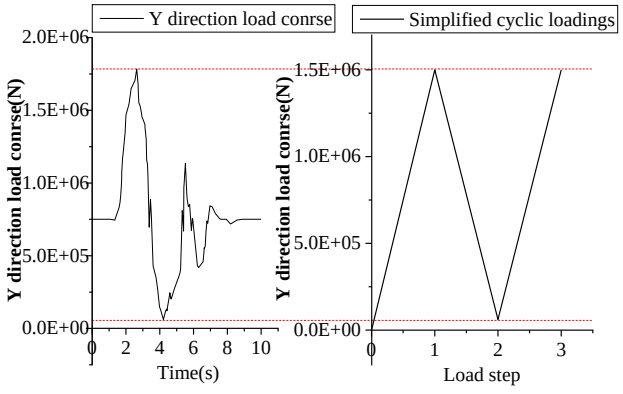

Fig. 7 Equivalent load in Y direction at left rear suspension

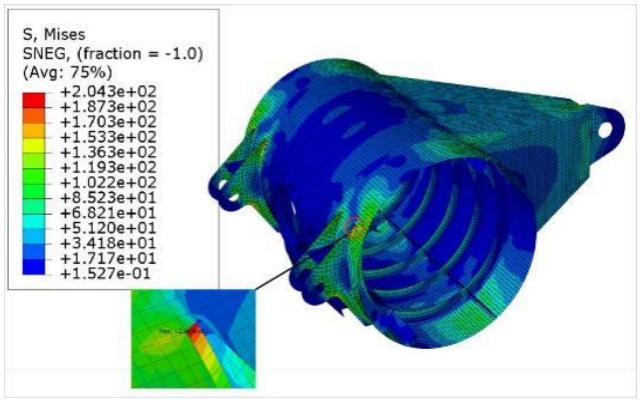

a

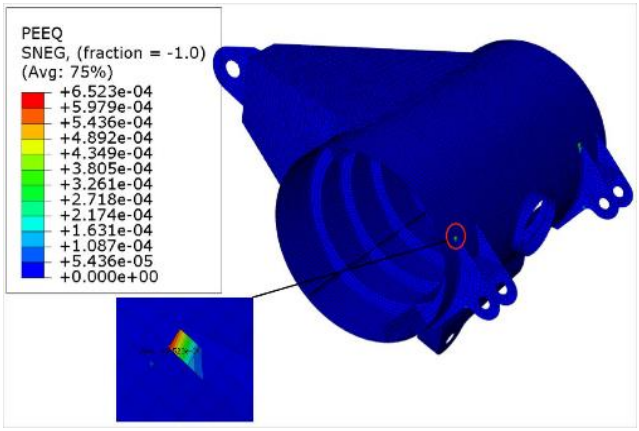

b

Fig. 8 Stress and strain contour on the surface of 17% slope turning under full load: a) stress distribution; b) strain distribution

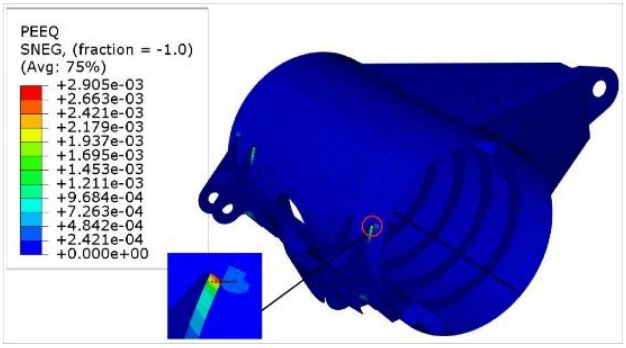

a

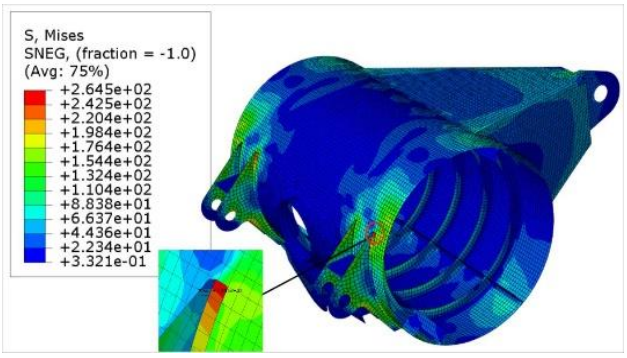

b

Fig. 9 Stress and strain contour on the surface of potholed pavement under full load: a) stress distribution; b) strain distribution

It can be seen from the Figs. 8 and 9. that the maximum stress was located at the root of ear plate in right rear suspension support, and reached around 264 MPa on the surface of potholed pavement under full load, as well as the equivalent plastic strain. And the crack started from the root of the ear plate in right rear suspension support as well, as shown in Fig. 10, which showed that the calculation accuracy of finite element analysis for the welded rear axle housing under equivalent loads was reasonable.

According to the Eqs. (1) – (3) and the stress and strain hysteresis loop at dangerous points, the fatigue life of welded rear axle housing could be determined, as shown in Table 2. The minimum lifetime was 14017 cycles, and located at the root of ear plate in left rear suspension support, while the root of ear plate in right rear suspension only had 14739 cycles as well. Usually, the mining dump truck ran ten cycles every day, and then it meant that the welded rear axle housing could only work for around four years. The predicted results agreed well with the engineering practical data, however, it did not meet the requirement of design and usage and optimization design was needed.

Fig. 10 Cracks at root of the ear plate in right rear suspension support

3.3. Fatigue life prediction

According to the stress and strain history from the simulated results, the hysteresis loop with stress and equivalent plastic strain at the dangerous point the surface of potholed pavement under full load was obtained, as shown in Fig. 11. The plastic strain energy density was the area of closed hysteresis loop, while the elastic strain energy density was related with the maximum positive tensile stress.

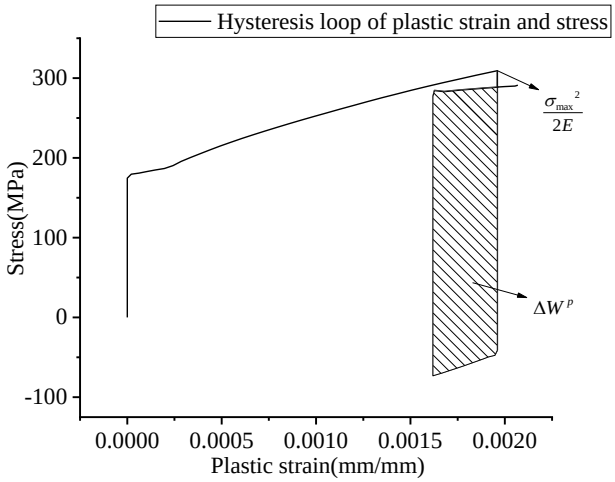

Fig. 11 Stress and strain hysteresis loop at dangerous point

Table 2

Fatigue life prediction of dangerous points

Dangerous point	Strain energy density	Horizontal surface	17% slope turning	Potholed pavement	Total strain energy density, MJ/m^3	Fatique life, cycle
Root of ear plate in left rear suspension	Elastic part	0.08236	0.11874	0.22773	0.546641	14017
	Plastic part	0	0	0.11781		
Root of ear plate in right rear suspension	Elastic part	0.08263	0.11804	0.22184	0.53036	14739
	Plastic part	0	0	0.10786		

4. Optimization design

4.1. Construction of optimization function

The rear axle housing was welded by four kinds of thickness plates, and the life expectancy was related with the thickness of plate. In order to improve the minimum fatigue life of welded rear axle housing, the optimization function could be described as:

$$Max: f(x) = N(x_1, x_2, x_3, x_4), \quad (5)$$

where: x_1 is the wall thickness of cylinder; x_2 is the thickness of the left and right ear plate; x_3 is the thickness of the tripod plate; x_4 is the thickness of the inner rib plate.

In order to build the relationship between the lifetime of welded rear axle housing and four design variables, the response surface method was utilized to the mathematical function. Then, the Latin Hypercube sampling method was firstly used to produce 20 groups of sample points for the design variables. The allowable variation range of variables was plus or minus 50%. After the sample points were obtained, the stress-strain responses at dangerous points under working conditions could be determined, and therefore the corresponding lifetime could be calculated according to the strain energy density model. Then, the results were shown in Table 3.

Table 3

Design variables and their response values

Sample points	Wall thickness of cylinder	Thickness of ear plate	Thickness of tripod plate	Thickness of rib plate	Total strain energy density, MJ/m^3	Fatique life, cycle
1	14.95	40.53	12.00	18.95	0.5687	13123.93
2	17.05	45.79	13.26	13.26	0.5794	12724.49
3	12.00	44.74	20.21	17.68	0.6070	11777.54
4	13.26	39.47	22.74	22.74	0.5639	13310.45
5	18.32	33.15	12.63	17.05	0.6132	11580.51
6	13.68	48.95	15.16	20.84	0.5122	15618.58
7	16.21	30.00	16.42	13.90	0.7159	8953.87
8	15.37	50.00	22.11	14.53	0.5589	13509.68
9	18.74	38.42	20.84	12.63	0.6248	11227.63
10	20.00	36.32	18.95	19.58	0.5352	14514.03
11	14.11	41.58	18.32	12.00	0.6825	9695.42
12	19.58	47.90	17.05	16.42	0.4866	17006.07
13	12.84	32.11	17.68	20.21	0.6595	10262.98
14	15.79	35.26	15.79	24.00	0.5516	13807.36
15	14.53	35.26	23.37	15.79	0.6668	10076.74
16	12.42	37.37	14.53	15.16	0.6904	9510.84
17	17.47	31.05	21.47	21.47	0.5958	12148.96
18	16.63	46.84	19.58	23.37	0.4556	18971.65
19	19.16	42.63	13.89	22.11	0.4674	18182.32
20	17.89	43.68	24.00	18.32	0.5116	15648.36

According to the design variables and response values, the second-order response surface function was chosen to construct the approximate model between plate thickness and lifetime, as shown in the following equation:

$$N(x) = 11589.86 - 353.88 * x_1 - 390.43 * x_2 + 147.14 * x_3 - 404.94 * x_4 - 14.51 * x_1^2 - 0.43 * x_2^2 -$$
$$-3.72 * x_3^2 - 5.84 * x_4^2 + 24.90 * x_1 * x_2 + 2.71 * x_1 * x_3 + 23.90 * x_1 * x_4 + 0.61 * x_2 * x_3 + 17.64 * x_2 * x_4 + 0.64 * x_3 * x_4, \quad (6)$$

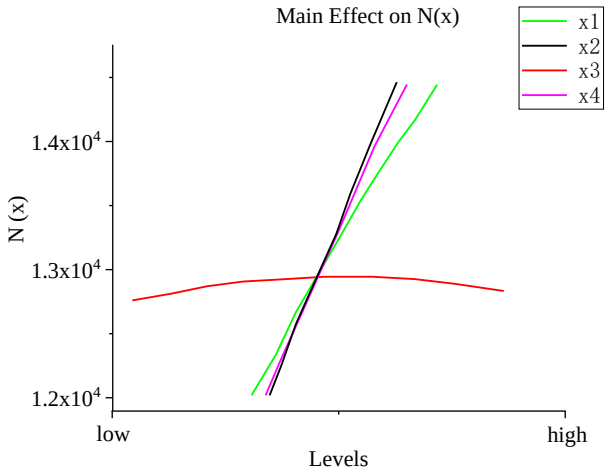

Fig. 12 Pareto diagram of design variables

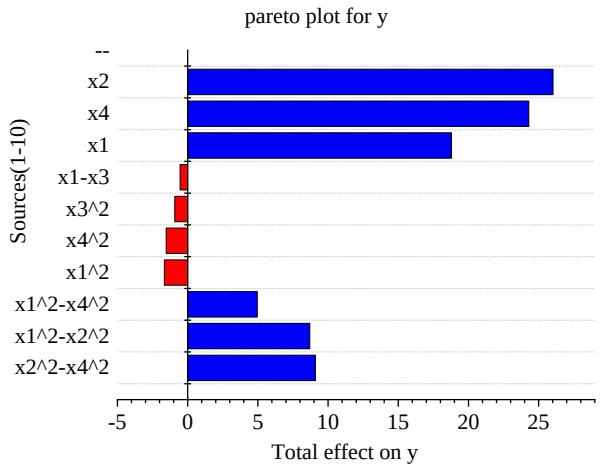

Fig. 13 Main effects of design variables

In order to figure out how the design variables have influence on the optimization objective, the Pareto diagram was shown in Fig. 12. It could be seen that the design variable x_2 had the biggest influence on the lifetime, which reached around positive 22%, and followed by the design variable x_4 and x_1. The quadratic term x_1^2 and x_4^2 had the opposite influence, which was around negative 2%. Similarly, the main effects on the optimization objective also showed that the design variable x_2, x_4 and x_1 produced most of influence, except the design variable x_3, as shown in Fig. 13. Moreover, the interaction effect between design variable x_1 and x_2 showed in Fig. 14 told that there was not

too much correlation between them. The response surface relationship between the wall thickness of cylinder and the thickness of the left and right ear plate appeared in non-linear function, as shown in Fig. 15.

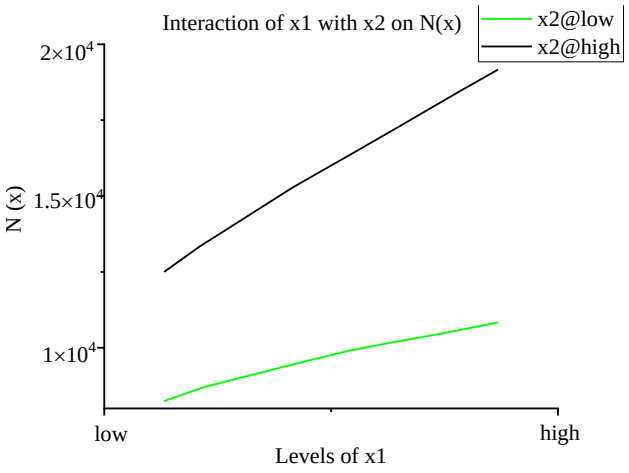

Fig. 14 Interaction effects of x_1 and x_2

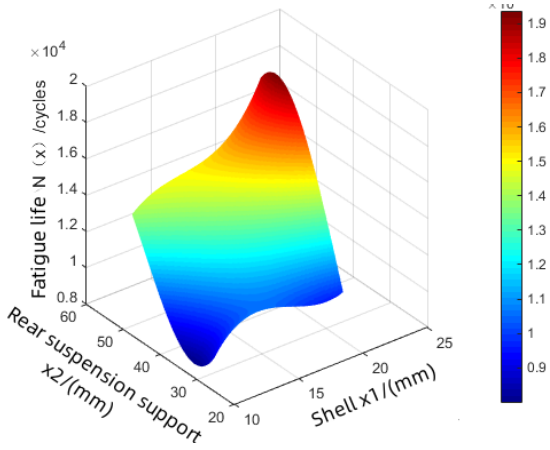

Fig. 15 Response surface relationship

4.2. Optimization design based on multi-island genetic algorithm

In this paper, based on multi-island genetic algorithm, the optimization calculation was performed in software ISIGHT. The number of sub-populations of this optimization was set as 10, the number of islands was 20, and the genetic algebra was 100 times. After 49 minutes of iterative calculation, the optimized plate thickness value was obtained, as shown in Table 4.

Table 4

Optimized results

Variate	Initial	Optimized
x_1, mm	16	20
x_2, mm	40	60
x_3, mm	18	16
x_4, mm	20	22
Minimum fatique life, cycles	14242	26669

It could be clearly seen that the thickness of cylinder, ear plate and inner rib plate were all increased to 20 mm, 60 mm and 22 mm, respectively, while the thickness of tripod plate was reduced to 16 mm. Even though the weight of welded rear axle housing slightly added, the minimum endurance life was increased from 14242 cycles to 28438 cycles, namely improved form 3.9 years to 8.2 years. The minimum fatigue life in the optimized structure could meet the design requirement, which normally was 8 years.

5. Conclusion

In this paper, an energy-based fatigue life prediction method and anti-fatigue optimization design of welded rear axle housing in a mining dump truck were carried out. The accuracy of finite element model for the welded rear axle housing was firstly testified by the experimental work, and the simulated results agreed well with the tested data. Based the suggested energy-based model, the fatigue life assessment was conducted, and the minimum life span was found to be insufficient. Then, the optimization function of welded rear axle housing was constructed by the response surface method, and the relationship between the design variables and optimization objective was analyzed. Based on the multi-island genetic algorithm, the global optimization was performed. Finally, the minimum fatigue life of the optimized rear axle housing was doubled.

Acknowledgments

This work is supported by the Major Foundation of Hunan Education Department (Grant No.:21A0362) and the Natural Science Foundation of Hunan Province (Grant No.:2021JJ50042 and 2022JJ50050) and Hunan Graduate Research Innovation Project (Grant No.: CX20220850).

References

1. **Mi, C. J.; Liu, J. D.; Xiao, X. W.;** et al. 2019. Interval multi-objectives optimization of electric wheel dump truck frame based on blind number theory, Applied Sciences 9(20). https://doi.org/10.3390/app9204214.
2. **Ma, X. K.; Gu, Z. Q.; Mi, C. J.; et al.** 2020. Weak ternary interval evaluation of fatigue life and its application to mining dump truck, J. Fatigue & Fracture of Engineering Materials & Structures 43(10): 2441-2454. https://doi.org/10.1111/ffe.13314.
3. **Mi, C. J.; Huang, Z. L.; Li, W. T.;** et al. 2021. Multi-objectives optimization design of A-type frame in an Electric mining dump truck considering multi-source uncertainties based on the interval method, Mechanika 27(2): 168-174. https://doi.org/10.5755/j02.mech.24939.
4. **Hrabowski, J.; Ummenhofer, T.** 2019. Low cycle fatigue of welded very and ultra-high strength steels, Procedia Structural Integrity 19: 259-266. https://doi.org/10.1016/j.prostr.2019.12.028.
5. **Zamzami, I. A.; Davison, B.; Susmel, L.** 2019. Experimental fatigue curves to perform the fatigue assessment of aluminium-to-steel thin welded joints, Procedia Structural Integrity 18: 255-261. https://doi.org/10.1016/j.prostr.2019.08.161.
6. **Wu, Y. P.; Liu, H. B.; Chen, Z. H.;** et al. 2020. Study on low-cycle fatigue performance of Aluminum alloy temcor joints, KSCE Journal of Civil Engineering 24(2): 195-207. https://doi.org/10.1007/s12205-020-0554-8.
7. **Zhao, H. S.; Lie, S. T.; Zhang, Y.** 2018. Fatigue as-

sessment of cracked pipes with weld misalignment by using stress intensity factors, International Journal of Fatigue 116: 192-209. https://doi.org/10.1016/j.ijfatigue.2018.06.030.
8. **Lie, S. T.; Zhao, H. S.** 2018. Fracture analysis of load-carrying cruciform fillet welded joints with multiple cracks, Engineering Fracture Mechanics 193: 32-46. https://doi.org/10.1016/j.engfracmech. 02.027.
9. **Jahed, H.; Varvani-Farahani, A.** 2005. Upper and lower fatigue life limits model using energy-based fatigue properties, International Journal of Fatigue, 28(5): 467-473 https://doi.org/10.1016/j.ijfatigue.2005.07.039.
10. **Pakandam, F.; Varvani-Farahani, A.** 2010. A comparative study on fatigue damage assessment of welded joints under uniaxial loading based on energy methods, Procedia Engineering 2(1): 2027-2035 https://doi.org/10.1016/j.proeng.2010.03.218.
11. **Mi, C.; Gu, Z.; Yang, Q.;** et al. 2012. Frame fatigue life assessment of a mining dump truck based on finite element method and multibody dynamic analysis, Engineering Failure Analysis,23(4): 18-26. https://doi.org/10.1016/j.engfailanal.2012.01.014.
12. **Zheng, S.; Kai, C.; Wang, J. ;** et al. 2015. Failure analysis of frame crack on a wide-body mining dump truck, Engineering Failure Analysis 48: 153-165. https://doi.org/10.1016/j.engfailanal.2014.11.013.
13. **Mi, C. J.; Li, W. T.; Wu, W. G. ;** et al. 2019. Fuzzy fatigue reliability analysis and optimization of A-type frame of electric wheel dump truck based on response surface method, Mechanika 25(1): 44-51. https://doi.org/10.5755/j01.mech.25.1.21726.
14. **Topaç, M. M.; Günal, H.; Kuralay N. S.** 2008. Fatigue failure prediction of a rear axle housing prototype by using finite element analysis, Engineering Failure Analysis 16(5): 1474-1482. https://doi.org/10.1016/j.engfailanal.2008.09.016/
15. **Shao, Y. M.; Liu, J.; Mechefske, C. K.** 2011. Drive axle housing fatigue analysis of a mining dump truck based on the load spectrum, Engineering Failure Analysis (18): 1049-1057. https://doi.org/10.1016/j.engfailanal.2010.12.023.
16. **Roostaei, A. A.; Pahlevanpour, A.; Behravesh, S. B.;** et al. 2018. On the definition of elastic strain energy density in fatigue modelling, International Journal of Fatigue 121: 237-242. https://doi.org/10.1016/j.ijfatigue.2018.12.011.
17. **Zhang, X. P.; Wang, D. F.; Kong, D. W.;** et al. 2022. The anti-fatigue lightweight design of heavy tractor frame based on a modified decision method, Structural and Multidisciplinary Optimization 65(10): 1-15. https://doi.org/10.1007/s00158-022-03385-9.
18. **Z G. Hu, P Zhu, J. Meng.** 2010. Fatigue properties of transformation-induced plasticity and dual-phase steels for auto-body lightweight: Experiment, modeling and application[J]. Materials & Design, 31(6):2884-2890. https://doi.org/10.1016/j.matdes.2009.12.034.

J. H. Liu, C. Zhang, D. Zhang, X.H. Liu, X. L. Hu, D. J. Zhang, C. J. Mi

AN ENERGY-BASED ANTI-FATIGUE OPTIMIZATION DESIGN METHOD OF WELDED REAR AXLE HOUSING IN A MINING DUMP TRUCK

S u m m a r y

In order to improve the life expectancy of the rear axle housing in a mining dump truck, an energy-based anti-fatigue optimization design method was presented in this paper. The finite element model of rear axle housing was constructed and testified by the experimental data. The load history was obtained through multi-body dynamics analysis, and the multi-load step nonlinear finite element analysis was carried out to obtain the stress-strain response under different working conditions. The strain energy density method was used to evaluate the fatigue life of rear axle housing, and the results showed that its fatigue endurance was insufficient. Then, the lifetime of the most dangerous point was taken as the optimization objective, and the different plate thickness was considered as the design variables. The approximate model was constructed based on the response surface method, and the anti-fatigue optimization design was finally conducted on the bearing structure through the multi-island genetic algorithm. The minimum fatigue life of optimized rear axle housing was doubled.

Keywords: anti-fatigue optimization; rear axle housing; strain energy density; approximate model.

Received September 29, 2022
Accepted August 2, 2023